5-2022

Cas9 gRNA and Homologous Recombinant Plasmid Integrate Inducible HA-N-ICER in the AAVS1 Locus of SK-MEL-24 Cells

Douglas Job

Abstract

Melanoma is one of the most aggressive forms of cancer and is prone to metastasis. Once melanoma metastasizes, it is difficult to treat as patients often become immune to MAPK inhibitors and other therapeutic agents. Small molecules, such as immune checkpoint inhibitors, have demonstrated success as an adjunct to melanoma treatment. As a small, 18kDa molecule with tumor suppressing properties, research using ICER continues to provide positive anti-tumor effects. ICER regulates cAMP-induced transcription as a powerful, dominant-negative transcriptional repressor. Recent research demonstrated that the fusion tag hemagglutinin (HA), when fused to ICER's N-terminus, increased ICER's half-life and apoptotic activity in SK-MEL-24 cells. If a stable, inducible HA_N-ICER cell line is established, much more research will be able to take place to further understand the role of ICER in melanoma cells. Until now, a stable HA_N-ICER cell line has not been developed despite many efforts to accomplish this in the laboratory. Here, it was demonstrated that co-transfection with a homologous recombination (HR) plasmid and a Cas9 gRNA plasmid which targets the AAVS1 safe harbor locus were used to incorporate EGFP into the genome of SK-MEL-24 cells as a proof of concept. Results were confirmed by fluorescent microscopy and Sanger sequencing data. Additionally, HA_N-ICER was integrated into the SK-MEL-24 cellular genome, and results were confirmed by western blot and immunocytochemistry (ICC).

MONTCLAIR STATE UNIVERSITY

CAS9 GRNA AND HOMOLOGOUS RECOMBINANT PLASMID INTEGRATE INDUCIBLE HA-N-ICER IN THE AAVS1 LOCUS OF SK-MEL-24 CELLS

by

Douglas Job

A Master's Thesis Submitted to the Faculty of

Montclair State University

In Partial Fulfillment of the Requirements

For the Degree of

Master of Science

May 2022

College of Science and Mathematics

Department of Biology

Thesis Committee:

[redacted]

Dr. Carlos A. Molina

Thesis Sponsor

[redacted]

Dr. Kirsten Monsen-Collar

[redacted]

Dr. Sandra Adams

Committee Member

CAS9 GRNA AND HOMOLOGOUS RECOMBINANT PLASMID INTEGRATE INDUCIBLE HA-N-ICER IN THE AAVS1 LOCUS OF SK-MEL-24 CELLS

A THESIS

Submitted in partial fulfillment of the requirements

For the degree of Master of Science

by

Douglas Job

Montclair State University

Montclair, NJ

2022

Acknowledgements

I thank God for helping me achieve this goal. I would also like to thank my incredible girlfriend, whose support throughout the graduate program has been instrumental; my family and friends for believing in me; Angelo and Dr. Molina for their expertise and continuous help throughout the research and thesis process; Dr. Monsen, who has helped me on many occasions throughout graduate school; all of my professors who kept me motivated through their passion for what they do; and an Anatomy and Physiology professor/MD I had a long time ago, who initially introduced me to molecular biology and advised that I seek it as a course of study.

TABLE OF CONTENTS

ABSTRACT……1

SIGNATURE PAGE……...2

TITLE PAGE.....3

ACKNOWLEDGEMENTS……...……..4

TABLE OF CONTENTS.....5

LIST OF FIGURES 6

INTRODUCTION……...7

MATERIALS AND METHODS……...14

RESULTS……..18

DISCUSSION……23

CONCLUSION……..28

BIBLIOGRAPHY……..……29

LIST OF FIGURES

Figure 1: Mechanism of CRISPR/Cas9 complex formation and DNA targeting activity…..……12
Figure 2: Snapgene® plasmid map depicting HA_N-ICER under the TRE3G promoter……15
Figure 3: Snapgene® plasmid map depicting the Cas9 gRNA……..16
Figure 4: Fluorescent microscopy showing images of SK-MEL-EGFP cells……...18
Figure 5: Western blot depicting HA_N-ICER expression……..19
Figure 6: Snapgene® sequence alignment of purified genomic EGFP with the plasmid DNA…20
Figure 7a: ICC performed on transiently transfected SK-MEL-390 cells (DAPI)…...…….21
Figure 7b: ICC performed on transiently transfected SK-MEL-390 cells …… …..…21
Figure 7c: ICC performed on SK-MEL-459B cells (DAPI)……...……...…22
Figure 7d: ICC perfomed on SK-MEL-459B cells……22

Introduction

The inducible cyclic-AMP early repressor (ICER) protein is a dominant negative transcriptional repressor and isoform of the *CREM* gene, and it responds to intracellular concentrations of cAMP by downregulating cAMP-induced transcription (Molina et al., 1993, Stehle et al., 1993). ICER has been shown to suppress cancerous cell growth *in vitro* as well as suppress tumor growth *in vivo* (Lamas et al., 1997; Razavi et al., 1998; Yehia et al., 2001). ICER weighs roughly 18kDa and has a simple leucine zipper structure (Poulkes et al., 1991; Ruchaud et al., 1997). The tumor-suppressing properties and its small size make ICER an attractive target for small molecule therapy.

It was previously demonstrated that ICER blocks DNA synthesis and cell cycle progression in the G2/M phases in AtT20 murine pituitary corticotroph cell lines and JEG-3 human choriocarcinoma cell lines (Lamas et al., 1997; Razavi et al., 1998). In the same studies, Lamas et al. (1997) and Razavi et al. (1998) demonstrated that exogenous expression of ICER in AtT20 cells repress cyclin A, a tightly regulated gene product expressed at the S and G2/M phases of the cell cycle. Another study found that ICER is the mechanism by which cAMP-induced apoptosis occurs in rat myeloid leukemia IPC-81 cells; the same study also mentioned it may inhibit cAMP-induced apoptosis, depending on nuclear ICER concentrations and when the apoptotic signal is initiated (Ruchaud et al., 1997). Apoptosis is a normal cellular response to tumorigenicity (Yonish-Rouach et al., 1991). If ICER is downregulated in the nucleus, disruption of cAMP -induced apoptosis will lead to tumor growth. ICER downregulation was observed in the LNCaP and DU 145 human prostate cancer cell lines; untreated cells barely express ICER, and they rapidly grow compared to cells either treated with cAMP or transfected with ICER (Yehia et al., 2001). Yehia et al. (2001) revealed that nude mice grafted with ICER-

expressing LNCaP cells either do not grow tumors or grow smaller tumors compared to nude mice grafted with only LNCaP cells.

Additional research indicates that cAMP stabilizes ICER expression in JEG-3 and AtT20 cells through inhibition of the MAPK Erk1 protein kinase, which phosphorylates ICER at serine 41 and targets it for ubiquitination (Yehia et al., 2001). Site-directed mutagenesis of serine 41 to alanine 41 results in the increased half-life of ICER. Furthermore, CDk1 phosphorylates ICER on Ser 35 and Ser 41 during mitosis in prostate cancer cells, which leads to ICER ubiquitination. ICER monoubiquitination results in its transportation out of the nucleus, where it is rendered functionally inactive. Yehia et al. (2001) also found that ICER is polyubiquitinated at internal lysine residues, which is a signal for proteasomal degradation. Site-directed mutagenesis of 11 internal lysine residues to arginine increases ICER expression, as lysine is a substrate for an E3 ligase ubiquitination reaction (Hershko & Ciechanover, 1998). The data suggest that ICER's half-life and nuclear concentrations are important in regulating cAMP-mediated apoptosis in oncogenic cells, and that ICER phosphorylation and ubiquitination disrupt its ability to inhibit tumor growth. It would follow from these experiments that modifying exogenous ICER to prevent its unwanted phosphorylation and ubiquitination is a top consideration for its use as a small molecule drug in cancer treatment.

Recent experiments investigating post-translational modifications of ICER found that the availability of ICER's N-terminus directly affected its half-life and efficiency in repressing cAMP-mediated transcription (Cirinelli et al., 2022). This study tracked ICER's half-life using a hemagglutinin (HA) fusion tag on either its N-terminus or C-terminus. It was found that the blocked N-terminus increases ICER's half-life and transcriptional repression activity. Cirinelli et al. (2022) also demonstrated that the HA_N-ICER increases apoptotic activity as measured by

TUNEL assays in metastatic melanoma SK-MEL-24 cell lines. Increasing the apoptotic activity of a tumorigenic cell is a decisive goal in cancer research, and further studies are needed to elucidate ICER's role in apoptosis. Additionally, protein interactions involved in the ubiquitination of ICER were identified. The promising data found in SK-MEL-24 cells, where endogenous ICER expression is either minimal or absent, support further studies into its role in melanoma.

Melanoma is an aggressive form of skin cancer commonly caused by a *BRAF* V600E mutation (Davies et al., 2022). BRAF is a RAF isoform encoded by the *BRAF* oncogene which phosphorylates MEK1 and MEK2 as part of the MAPK pathway (Marais & Marshall, 1996). The *BRAF* V600E mutation leads to a constitutively active BRAF protein, which ultimately results in the loss of cell cycle regulation and cancer. Importantly, high intracellular levels of cAMP downregulate the MAPK pathway by interrupting the interactions between Raf and Ras proteins (Wu et al., 1993). Inhibiting the MAPK pathway prevents cell proliferation. However, cAMP's impact on the MAPK pathway may be cell-specific: for example, in PC12 neuronal cells, cAMP activates ERK1, ERK2 and Elk1 in Ras-independent pathways, leading to cell differentiation (Vossler et al., 1997). Additionally, *CDKN2A* mutations may also be found in melanoma. *CDKN2A* is responsible for the production of p16 and p14 proteins. In healthy cells, p14 prevents p53 degradation and p16 binds to cyclin proteins CDK4 and CDK6, which prevents progression through the cell cycle and thus regulates mitosis (Li, Poi, & Tsai, 2011). The combination of *BRAF* and *CDK2NA* mutations are common in metastatic melanoma.

In 2022, the American Cancer Society (ACS) predicts that in the US, nearly 99,780 new cases of melanoma will be diagnosed and 7,650 will die from it (ACS, 2022). Advanced melanoma is characteristically resistant to chemotherapy, as patients either have or develop

resistance to MAPK and BRAF inhibitors during treatment. Patients often require different cocktails of immunotherapeutic and chemotherapeutic drugs, since multiple mutational or non-mutational events may also occur downstream of activating extracellular signals which render a single drug ineffective (Helmbach et al, 2001; Winder & Virós, 2018; Tripathi et al., 2020). There are numerous avenues of research which concentrate on immune checkpoint inhibitors, but there is a gap in the literature pertaining to how transcription factors in the cAMP signaling pathway can be studied in melanoma research (Chacon et al., 2021). Healey, Crow and Molina (2013) found that ICER inhibits the growth of Ras-mediated melanoma R545 cells on soft agar, and ICER also prevents melanoma genesis in SCID mice grafted with ICER-expressing R545 cells. However, R545 cells were from a murine cell line, and a better model representative for melanoma in humans would incorporate human melanoma cell lines. In order to accomplish this, a stably transfected human SK-MEL-24 melanoma cell line was generated.

Transfection introduces exogenous genetic material without a viral vector to a cell. Since DNA has a negatively charged phosphate backbone, it is not readily taken up by the cell's negatively charged plasma membrane. The DNA must be encapsulated in a hydrophobic vessel, cationic delivery system, or combination thereof which enables the DNA to pass into the cytoplasm (Kim & Eberwine, 2010). Stable transfections offer the advantage of conferring genetic integration of a gene of interest (GOI) to a host cell, thereby ensuring parental cells will pass on the GOI to daughter cells. In order to confirm the cell successfully integrated the DNA into its genome, reporter genes such as EGFP and drug selection markers like puromycin resistance are incorporated into the plasmid. Cells that have integrated the GOI will fluoresce and have resistance to puromycin, whereas cells that did not integrate the GOI will not fluoresce and will be killed by the puromycin. In this thesis, an EGFP control was used in a plasmid of its

own, while the protein hemagglutinin (HA) tag was fused to the N-terminus of ICER in another plasmid. Puromycin selection was performed on both the EGFP and HAN-ICER plasmids.

Additional methods have been developed to increase transfection efficiency in the lab. Cas9 has been used in co-transfection experiments with great efficiency to integrate a GOI into a precise location within a genome (Liang et al., 2015). Cas9 is a CRISPR-associated endonuclease made up of a sequence recognition domain and a nuclease domain, and it is found in a Type II CRISPR/Cas system (Nishimasu et al., 2014). In general, a CRISPR/Cas system is composed of palindromic repeats of 20 to 50 nucleotides divided by short spacer sequences, downstream from a leader sequence, in a locus adjacent to *cas* genes. The repeats are highly conserved but may differ depending on the CRISPR loci (Kunin, Sorek, & Hugenholtz, 2007). The short spacer sequences are similar to sequences found in viral genomes, and it was discovered that bacteria and archaea use CRISPR/Cas to cleave invading genetic material, termed protospacers. Then CRISPR/Cas integrates protospacers into the spacer sequences and the cell develops immunity to the invading virus (Barrangou et al., 2007; Bolotin et al., 2005; Brouns et al., 2008; Jinek et al., 2012; Wiedenheft et al., 2012). The recognition of 5' or 3'-flanking protospacer adjacent motifs (PAMs) is essential to this process (Bolotin et al., 2007). Upon bacteriophage invasion in a Type II CRISPR/Cas system, the CRISPR locus is transcribed. Non-coding short *trans*-activating CRISPR RNAs (tracrRNAs) base-pair with the elongated pre-crRNA, form complexes with Cas9, the complexes are cleaved by RNase III, and mature complexes ready to cleave invasive DNA are released (Bolotin et al, 2005; Brouns et al., 2008; Deltcheva et al., 2011; Jinek et al., 2012; Lino et al., 2018; Wiedenheft et al., 2012). The crRNA sequence is homologous to one strand of the phage DNA while the tracrRNA binds to the second strand, and Cas9 forms double-strand breaks near the PAM sequences using RuvC- and HNH-

like nuclease domains (Deltcheva et al., 2011; Gasiunas et al., 2012; Lino et al., 2018; Sapranauskas et al., 2011) (Figure 1).

The understanding of CRISPR/Cas has led to revolutionary developments in the laboratory, as gene-editing using engineered CRISPR/Cas systems is effective and easier to use than previous methods (Javed et al., 2018; Lino et al., 2018). Based on the tracrRNA and crRNA requirements for Cas9-mediated DNA cleavage, synthetic guide RNA (gRNA) compatible with Cas9 was developed and it was demonstrated that the Cas9/gRNA combination successfully targeted the GFP region within a plasmid (Jinek et al., 2012).

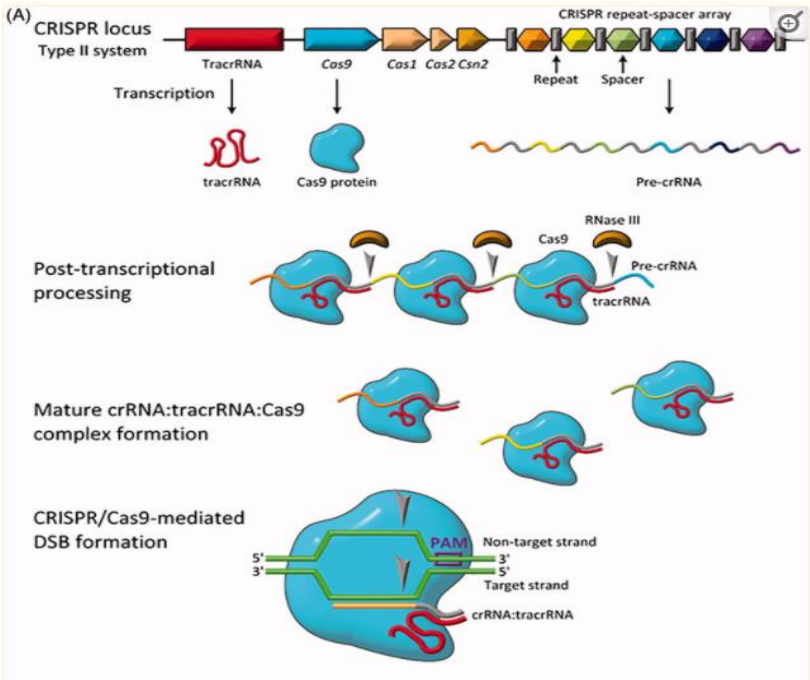

Figure 1. Mechanism of CRISPR/Cas9 transcription, processing, complex formation and DNA targeting (Lino et al., 2018).

Cas9 and synthetic gRNA enable accurate targeting of specific genetic loci in host genomes as well as plasmids to increase the efficiency of gene-editing and transfection experiments. However, random integration or off-target effects may occur during transfection, and researchers must use discretion when identifying the target gene locus. The AAVS1 safe

harbor locus describes a region on chromosome 19 in the human genome where the adeno-associated virus (AAV) inserts its DNA (Kotin, Linden, & Berns, 1992). AAVS1 is termed a safe harbor because modifications in this area of the genome do not result in observable cellular changes or disruptions to essential cellular systems. DNA in this locus may therefore be targeted with Cas9 gRNA and repaired via homologous recombination (HR), where an HR plasmid containing the desired transgene will safely integrate into the host genome.

Until today, a stable inducible ICER cell line was unable to be produced in SK-MEL-24 cells for reasons that are currently not clear. It is thought that a disruption in cell signaling or exogenous gene silencing takes place soon after transfection which causes the cells to undergo apoptosis. Here, a stable inducible EGFP-only cell line was generated in SK-MEL-24 cells (referred to as SK-MEL-EGFP) via co-transfection, as proof of concept using a Cas9 gRNA plasmid and a tetracycline-inducible HR plasmid. The plasmids were then used to stably transfect SK-MEL-24 cells with HA_N-wildtype ICER (SK-MEL-459). My hypothesis is that gene integration occurs in the AAVS1 safe harbor locus via homologous recombination of the donor plasmid, and HA_N-ICER is expressed when the cells are exposed to doxycycline.

Materials and Methods

Cells, Cell Culture, and Transfection

SK-MEL-24 human melanoma cells were purchased from ATCC® and cultured with Eagle's Minimum Essential Medium (EMEM),15% heat-inactivated Fetal Bovine Serum (HI-FBS) and Pen Strep (5.0mL P/S per 500.0mL EMEM) in a 75 cm^2 culture flask until 80% confluency. To split the cells, media was aspirated, and flask was rinsed with 5.0mL phosphate buffered saline (PBS). Trypsin (2.0mL 0.25%) was added to the flask which was then placed in a 37.0°C incubator for 5 minutes. EMEM/15% Tet-free FBS plus P/S (18.0mL) was added to the culture flask after incubation. 900.0uL aliquots were dispensed evenly in a 6-well 10mm^2 plate. Cells were transferred to a 37.0°C incubator and incubated for 24 hours, until 80% confluency. Cells were then removed from the incubator and media was replaced with 2.0mL EMEM plus Tet-free 15% FBS. Cells were transfected using the Promega Fugene® HD Transfection Reagent. Tet-free 15%FBS/EMEM (72.0µL), 8.0µL Fugene® HD, 10.0µL (0.1µg/µL) Tet-on®3G-HA_N-zfICERwt-AAVS1-HR plasmid, and 10.0µL (0.1µg/µL) All-in-One Cas9 SmartNuclease™ EF1-hspCas9-H1-AAVS1-gRNA plasmid (System Biosciences) were added to Eppendorf tubes (plasmid maps can be seen in Figure 2 and Figure 3). The EGFP control group was transfected as described with the Tet-on®3G-EGFP-AAVS1-HR (figure not shown) and EF1-hspCas9-H1-AAVS1-gRNA plasmids. Eppendorf tubes sat at room temperature for 15 minutes and transfection solution was pipetted equally into each well. Cells were incubated at 37.0°C overnight. Media was aspirated and replaced with 2.0mL EMEM/P/S and 15% Tet-free FBS.

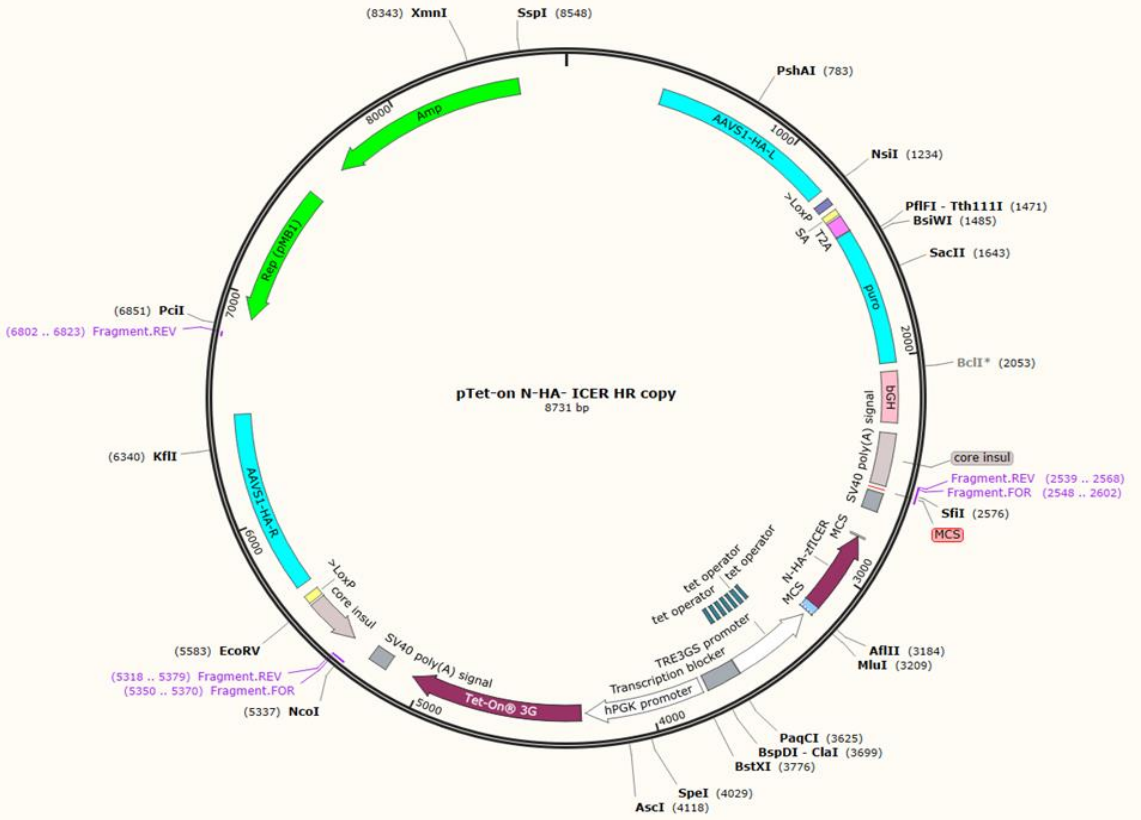

Figure 2. Snapgene® plasmid map depicting HA_N-ICER under the TRE3G promoter. The Tet-on® 3G protein changes its conformation after binding with doxycycline and then binds the TRE3G promoter to induce transcription.

Puromycin Selection

Cells were recovered approximately 10 days post-transfection. Puromycin (10.0mg/mL) was diluted 1:10 with deionized water (dH_2O) and then added to 10.0mL EMEM/15% Tet-free FBS, for a final concentration of 0.5µg/mL puromycin. Cells were removed from the incubator, media was aspirated and replaced with 2.0mL of the freshly made puromycin-containing media, and then incubated at 37°C for three days. Media was replaced every three days. Puromycin-resistant colonies developed after two weeks and were transferred to separate wells and allowed to grow for two passages before being split as described.

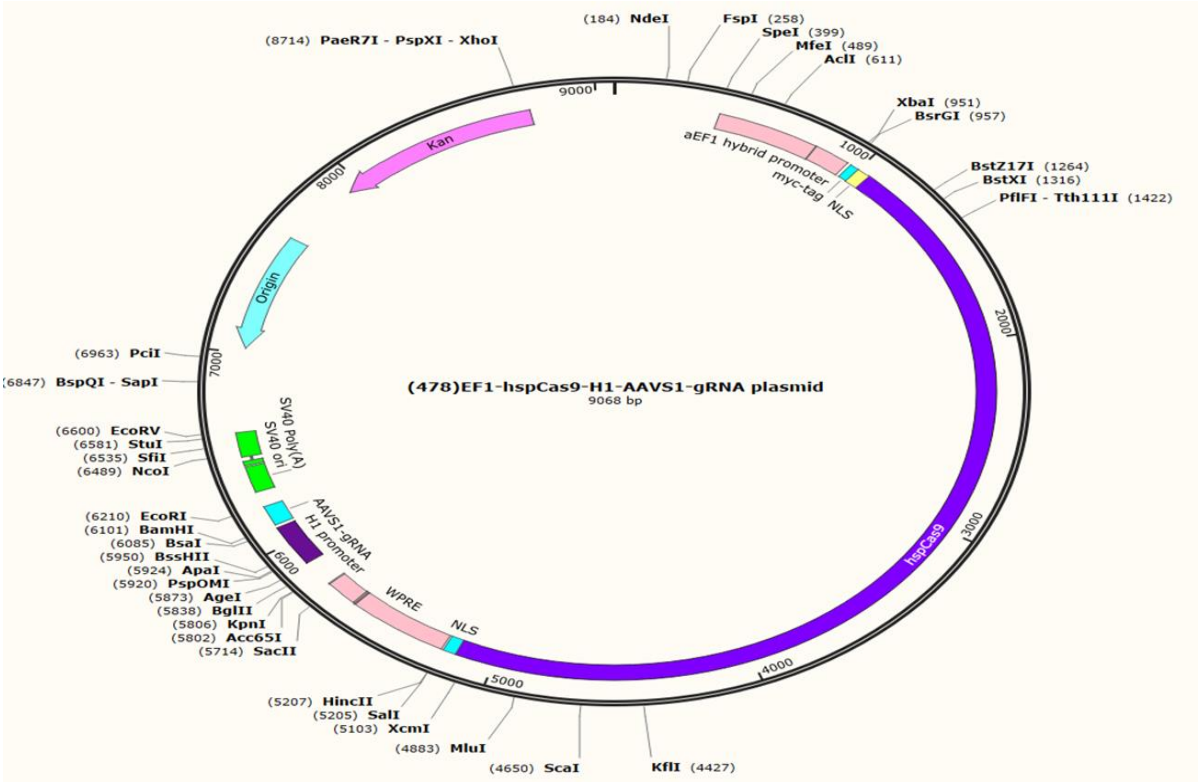

Figure 3. Snapgene® plasmid map depicting the Cas9 gRNA which targets and cleaves the AAVS1 locus.

Doxycycline Addition and Western Blot Analysis

Doxycycline [20.0µL (0.5µg/mL)] was added to wells containing SK-MEL-459B, SK-MEL-459C, and SK-MEL-EGFP5 (letters or numbers following the name of a cell line distinguish the identity of a selected colony). Water was added to separate wells of these cell lines as a negative control, and cells were incubated for 48 hours to achieve maximum induction. After the incubation period, cells were observed for fluorescence using the Nikon® Eclipse Ti inverted fluorescent microscope. Media was aspirated and cells were rinsed with PBS, then 500.0µL trypsin was added to each well. After cells incubated for three minutes, 1.0mL EMEM/15% HI-FBS +P/S was added to inactivate trypsin, cells were aliquoted into 1.5mL Eppendorf tubes and then centrifuged at 300g for 6 minutes. Samples for SDS-PAGE and Western Blot were prepared and performed as previously described (Yehia et al., 2001). Western blot detection was

performed using the LI-COR Odyssey CLx®. Rabbit monoclonal anti-HA antibodies were used as primary antibodies and were purchased from Invitrogen. IRDye® secondary antibodies were purchased from LI-COR for western blot imaging.

DNA Extraction and PCR

SK-MEL-459B/C and SK-MEL-EGFP1/5 cells were removed from wells and DNA was extracted per the Qiagen® DNeasy® Blood and Tissue Kit Quick-Start protocol. The forward HR primer selected for plasmid amplification was 5'-CCTCTGAACGCTTCTCGCTG-3' and the reverse HR primer was 5'-CGTACCACTTCCTACCCTCG-3'. PCR was performed according to DreamTaq Green PCR protocol (Thermo Scientific™).

Gel Electrophoresis and Sequencing

PCR-amplified DNA (10.0µL) was loaded into wells for 1.0% agarose gel electrophoresis. Gel was imaged using GelRed® Nucleic Acid Gel Stain under a UV light and the PCR product was sent to Genewiz from Azenta Life Sciences in South Plainfield, NJ for Sanger Sequencing. The forward primer included was 5'- CCTCTGAACGCTTCTCGCTG-3'.

Immunocytochemistry (ICC)

ICC was performed with anti-HA fluorescently tagged primary antibodies (anti-HA, mouse IgG1, clone 16B12, Alexa Fluor 594 [ThermoFisher Cat # A21288] at a dilution of 1:200). Cells were fixed and prepared as previously described (Cirinelli et al., 2022). After 100µL of primary antibody was applied to the samples, samples were incubated at 4°C overnight and then rinsed with PBS. DAPI [100µL (1.2µL/mL)] was then added. Samples sat for 30 minutes at room temperature before being rinsed with PBS and prepared for imaging with the Nikon® Eclipse Ti inverted fluorescent microscope.

Results

Doxycycline induced EGFP expression in SK-MEL-EGFP cells

Maximal induction of EGFP expression, as determined by the number of fluorescent cells, occurred approximately 48 hours after treatment with doxycycline (Figure 4), demonstrating that inducibility and plasmid integration were successful. Interestingly, the SK-MEL-EGFP1 cells stopped fluorescing (data not shown). Increasing doxycycline did not result in fluorescence. However, SK-MEL-EGFP5 cells continue to fluoresce.

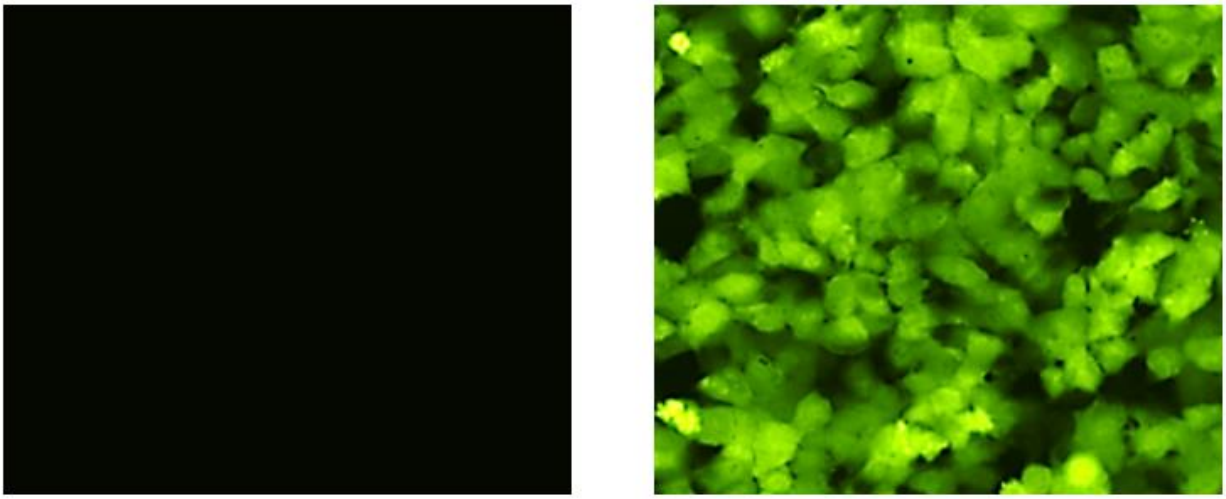

Figure 4. Fluorescent microscopy showing images viewed of SK-MEL-EGFP cells before (left) and after (right) addition of doxycycline (10X).

Western blot analysis demonstrated inducible HA_N-ICER expression

To identify inducible HA_N-ICER expression, a western blot was performed using anti-HA antibodies (Figure 5). Both 459B and 459C colonies expressed HA_N-ICER after doxycycline addition as seen in the approximate 22kDa band region in lanes 2 and 4. ICER runs on a western blot at a slightly higher molecular weight than its structural molecular weight of 18kDa, and the fusion HA tag adds approximately 1kDa to the overall molecular weight, both of which account for the observed molecular weight. The subdued HA_N-ICER bands at 22kDa do not appear in the negative control lanes, which demonstrate that doxycycline induced HA_N-ICER expression in

SK-MEL-24 cells. Additionally, 20.0µL of the 459B(+) and 459C(+) HA_N-ICER cell extracts were loaded, compared to 10.0µL volumes loaded in each of the other respective lanes. This was done as it was unknown how strong the HAN-ICER signal would be. Despite doubling the protein volume loaded into the lanes, HA_N-ICER expression appears subdued. Research into factors influencing HA_N-ICER expression in SK-MEL-24 cells is still new and more is expected to be learned. The expression signals in lanes 8 and 9 are greater than those appearing in 2 and 4 as the lanes were overloaded, in the event no HA_N-ICER bands appeared in lanes 2 and 4.

Theoretically, bands should not be visible in the EGFP lanes, as anti-EGFP antibodies were not used in this experiment. Mass spectrometry would need to be performed in order to identify background expression, but it is doubtful that any significant information would result which pertains to the scope of this experiment.

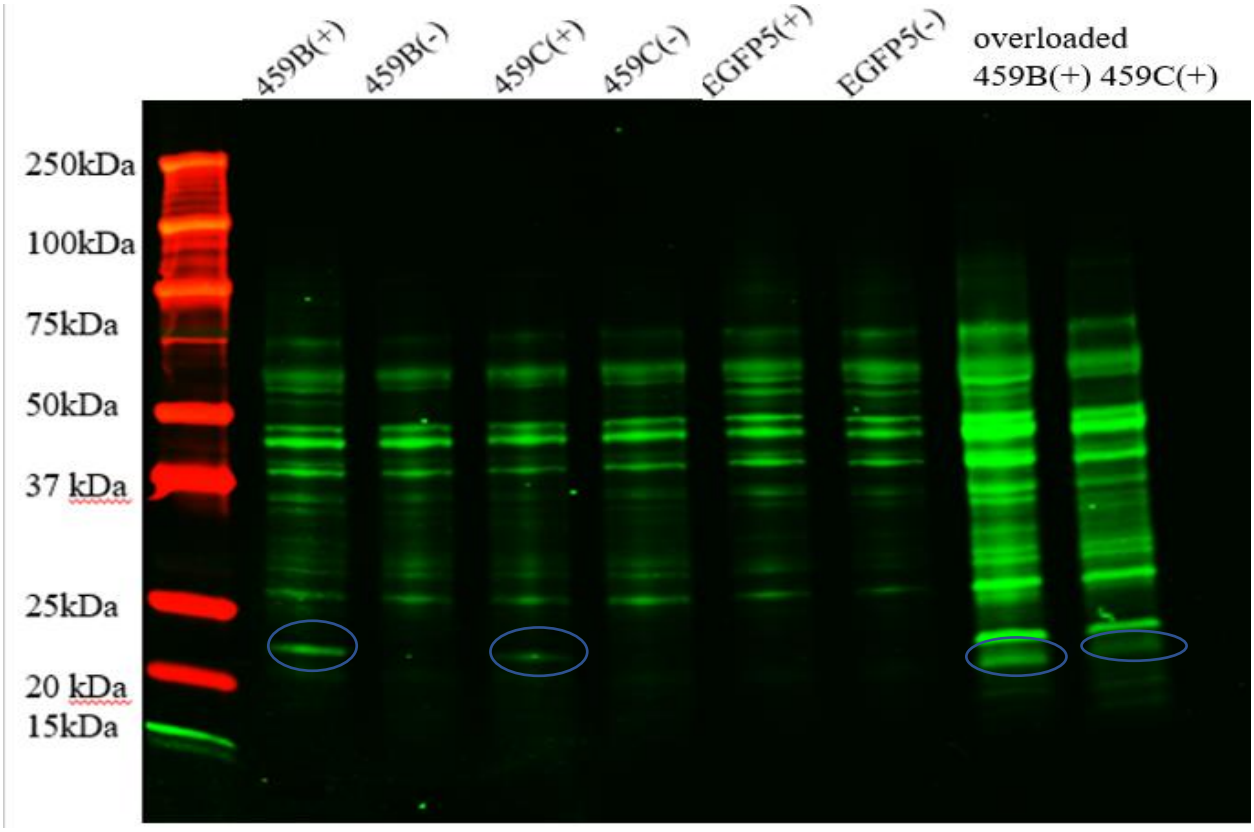

Figure 5. Western blot depicting HA_N-ICER expression in lanes 2, 4, 8, and 9.

Sanger Sequencing

Sanger sequencing data confirmed successful integration of the HR donor plasmid for EGFP5. The sequence for the extracted DNA was aligned with the HR plasmid DNA in Snapgene® software, as seen in Figure 6. There were three mismatches, no insertions, and no gaps in the alignment. However, these data do not confirm that the HR plasmid was integrated in the AAVS1 safe harbor locus, as primers would need to be selected for the nucleotide sequences flanking the genomic AAVS1 site. However, there was no abrupt cell death post-transfection, nor were any discernable morphological effects observed in the cells. Sequencing primers for genomic AAVS1locus were recently identified and designed, but sequencing results for 459B and 459C were not available by the time this thesis was completed.

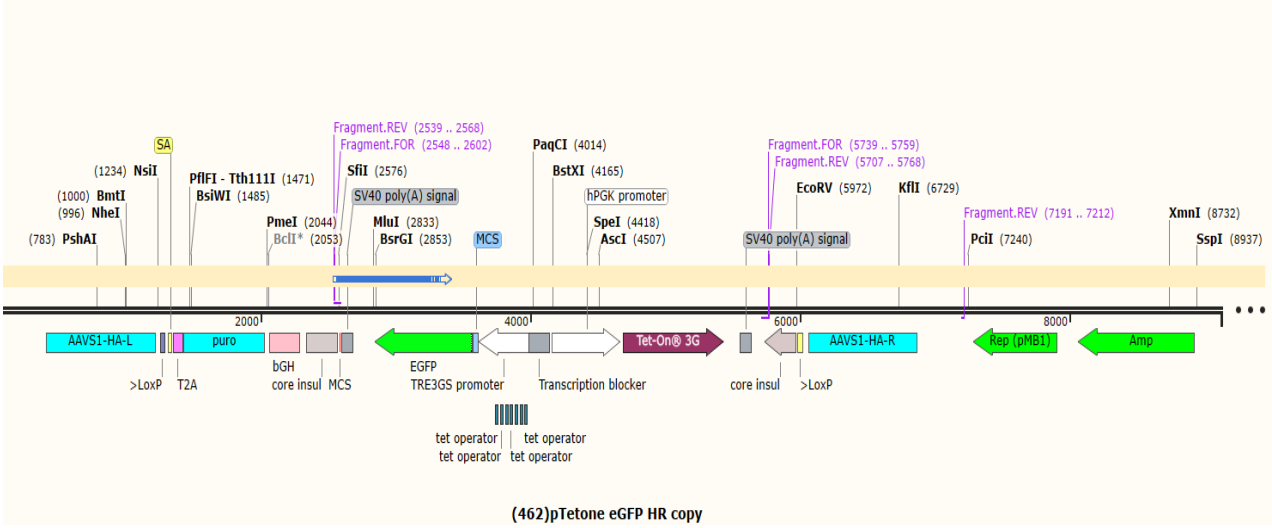

Figure 6. Snapgene® sequence alignment of purified genomic EGFP with the plasmid DNA. Purified genomic EGFP is represented by the blue arrow in the beige horizontal bar aligned above the linear plasmid map.

ICC demonstrates stable cell lines were generated with inducible HA_N-ICER

To compare stably transfected SK-MEL-459 (459B and 459C) colonies with transiently transfected HA_N-ICER colonies, 459B and 459C cell colonies were passaged for about one week before performing ICC. SK-MEL-24 cells were then transiently transfected with a pCMV

plasmid (SK-MEL-390). Transient transfections deliver exogenous DNA to the cell's nucleus, but it is not integrated into the genome; because of this, the DNA is eventually degraded, and progeny cells do not acquire the transfected genes. On the other hand, the stably transfected cells which were passaged were expected to demonstrate that all the cells express HA_N-ICER. The cells seen in Figure 7A were transiently transfected with HA_N-ICER and Figures 7B and 7C demonstrate 459B and 459C cells, respectively. DAPI was used as a counterstain to verify that cells, not random artifacts, were expressing fluorescently labeled HA_N-ICER. Clearly, HA_N-ICER expression in SK-MEL-390 cells is deficient compared to both 459B and 459C cell colonies.

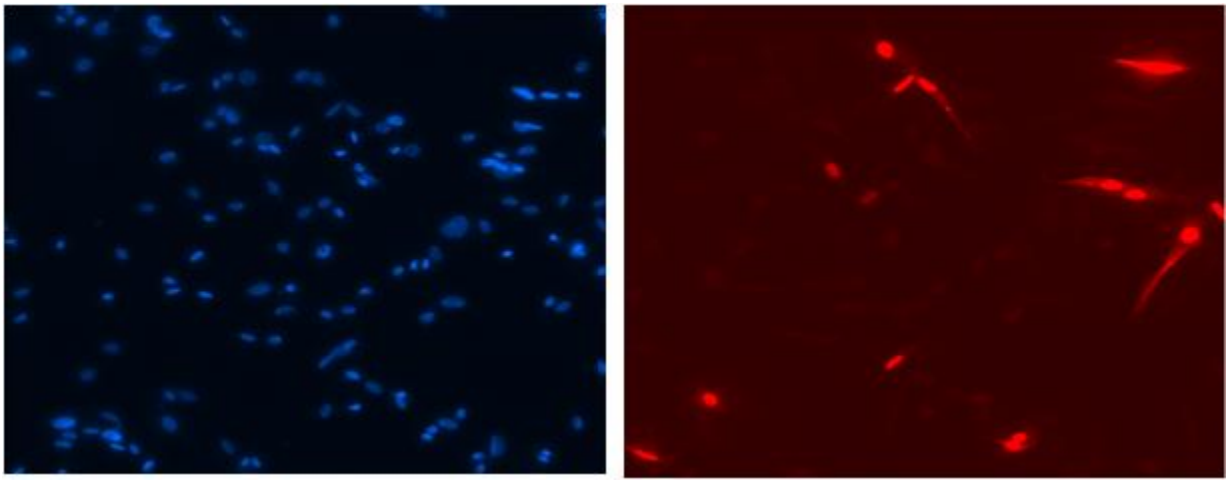

Figure 7A (left) and Figure 7B (right). ICC performed on cells transiently transfected with HA_N-ICER using a pCMV plasmid (10X). Transfection efficiency was calculated as the number of fluorescent cells divided by the total number of cells counted in a random field. DAPI image on the left is shown for reference.

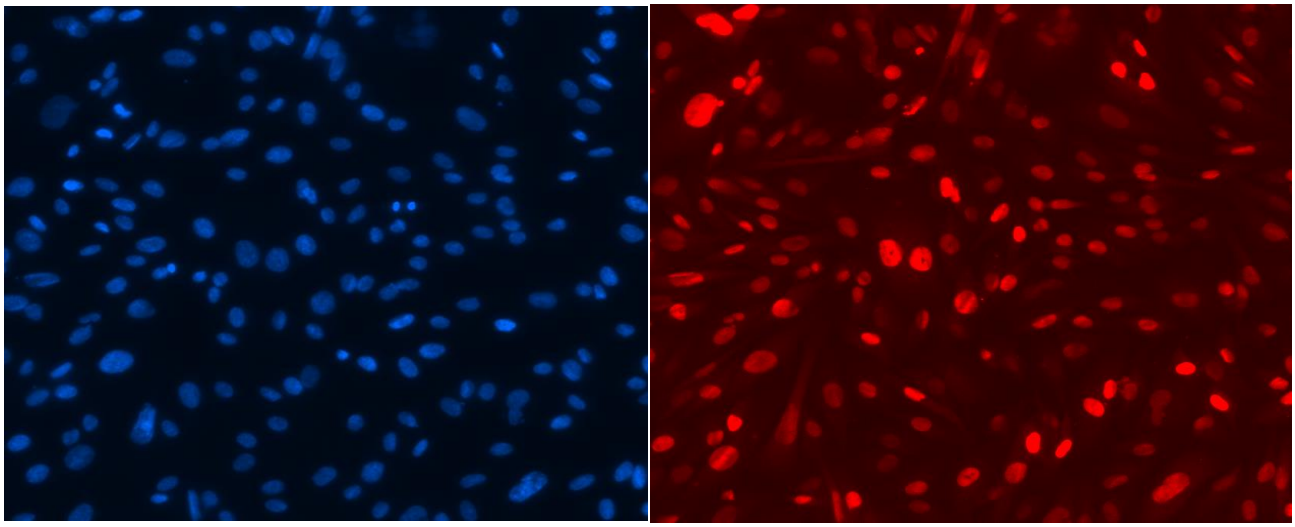

Figure 7C (left) and Figure 7D (right). 459B and 459C colonies were passaged for about one week before ICC was performed. Stable transfections with the HR plasmid and Cas9 gRNA in 459B and 459C HA_N-ICER colonies show that all cells are expressing HA_N-ICER (10X). DAPI image on the left is shown for reference.

Transfection efficiency was calculated as the number of fluorescent cells divided by the total number of cells in the microscopic field at 10X magnification. The transfection efficiency for the SK-MEL-390 cell colonies was about 21%. As the 459B and 459C colonies were passaged for about one week before staining and imaging, these results confirm that stable, puromycin-selected and dox-inducible HA_N-ICER cell lines were created.

Discussion

ICER expression decreases in active melanoma, as it is phosphorylated in the MAPK pathway, polyubiquitinated, and targeted to proteasomal degradation (Healey, Crow, & Molina, 2013). ICER is also monoubiquitinated and shuffled out of the nucleus into the cytosol, where its role as a transcriptional repressor is disabled (Mémin et al., 2011). Since endogenous baseline ICER expression is low in healthy melanocytes, melanoma cells express almost imperceptible levels of ICER. In experimenting with the HA tag on ICER's N-terminus and C-terminus to trace ICER expression in melanoma cells, it was discovered that the HA tag on the N-terminus reduces protein turnover (Cirinelli et al., 2022). In order to study the importance of HA_N-ICER expression in melanoma, stable cell lines were needed, but the transfection complexes used prior to these experiments resulted in rapid cell death. This thesis demonstrates that a stable cell line expressing HA_N-ICER was created, and these cells form the foundation for future HA_N-ICER experiments to follow.

Using the AAVS1 Cas9 gRNA plasmid and tet-inducible expression HR plasmid, the results of this study demonstrated that EGFP and HA_N-ICER were integrated into the genome of SK-MEL-24 cells. Doxycycline was able to induce the expression in SK-MEL-EGFP cells, as shown by fluorescent microscopy. It is interesting to note that after two cell passages, the SK-MEL-EGFP1 colonies stopped fluorescing. Krishnan et al. (2006) documented that epigenetic silencing of reporter genes occurred in H9c2-Fluc cells after months of cell passages, but reporter gene expression was recovered after exposing the cells to methyltransferase and deacetylase inhibitors, as well as a transcriptional activator. In SK-MEL-24 cells, two cell passages equate to approximately one week. If EGFP was epigenetically silenced within one week, methylation studies on the TRE3GS promoter should be performed in the transfected cells

via the bisulfite conversion method. This method relies on the conversion of unmethylated cytosine to uracil residues to confirm the degree of promoter methylation. On the other hand, methyltransferase and deacetylase inhibitors may also be used to see if there is an impact on the duration of EGFP expression. Epigenetic silencing would render doxycycline addition ineffective, because the promoter would be structurally obstructed after methylation. It was observed that doubling the amount of doxycycline to SK-MEL-EGFP cells did not cause the cells to regain fluorescence, and promoter methylation should be considered because of this observation. In addition, a duplicate experiment demonstrated that (data not shown) approximately 10% of SK-MEL-EGFP cells fluoresced before they were exposed to doxycycline, but not with the same intensity as if they were exposed to dox. This may indicate a leaky promoter, where EGFP was transcribed despite the absence of doxycycline, which is required to induce the conformational change in the transactivator necessary for *tet* operator binding in the promoter.

Expression of HA_N-ICER was observed in the Western blot, although the bands appeared weak. This may have been the result of protein loading; α-tubulin was not used to verify the amount of protein loaded in each lane. The relatively low intensity of the ~22kDa HA_N-ICER bands may indicate that silencing occurs to a small extent, but repeated experiments need to be performed to identify whether the band intensity increases, and α-tubulin must be used as a loading control. Many unidentified protein bands were also observed, although anti-HA and IRDye® were the only antibodies used in the procedure. Western blots may often generate images like this, and the causes may be the result of nonspecific antibody binding, secondary antibodies forming conjugates, or general interference. Cirinelli et al. (2022) demonstrated in their mass spectrometry data that there are many proteins which potentially interact with ICER,

such as UBR4 and NAA15, and it is likely that other proteins interact with ICER in different capacities. Most important in this Western blot is the presence of two 22kDa bands specific to lanes 2 and 4, which demonstrate HA_N-ICER expression. Additionally, it was concluded from the ICC results that the SK-MEL-459B and SK-MEL-459C colonies were stably transfected with HA_N-ICER, as after about two passages demonstrate in Figures 7C that all cells fluoresce upon exposure to anti-HA antibodies. Importantly, the cells continue to be passaged. Previous experiments were unsuccessful in maintaining ongoing cell viability. These results and observations support the hypothesis that HA_N-ICER integrated into the AAVS1 locus.

The sequencing results confirm that the EGFP5 plasmid was integrated into the SK-MEL-24 genome. Although it was unable to be verified that the HR plasmid integrated in the AAVS1 locus (as compared to a random locus), the principle behind homologous recombination supports the hypothesis that the HR plasmid was inserted into the AAVS1 locus. Homologous recombination does not rely on restriction sites; rather, any extended region of DNA with enough similarity to another long strand of DNA can initiate homologous recombination after a dsDNA break. In this experiment, Cas9 gRNA (synthetic crRNA fused to tracrRNA) and an HR plasmid were used. The gRNA recognizes the AAVS1 locus and forms a complex with Cas9, which then causes a dsDNA break. The HR plasmid serves as the repair template for homologous recombination at the AAVS1 locus, as the flanking ends of the HR plasmid are homologous to the flanking ends of the genomic AAVS1 DNA. EGFP, located in between the flanking arms of the HR plasmid, was then introduced into the cell's genome. A limitation to this thesis was that the flanking sequences of the AAVS1 locus in the genome were recently identified and primers were designed, but sequencing has yet to be performed. Sanger sequencing will be needed to confirm that the EGFP and HA_N-ICER sequences were inserted into the target AAVS1 locus.

Importantly, experiments with the SK-MEL-459 cell lines will shed light on the interactions between UBR4 and ICER; UBR4 was found to ubiquitinate ICER according to the N-end rule proteasome pathway (Cirinelli et al., 2022). Cirinelli et al. (2022) also demonstrated that NAA15 interacts with ICER and influences its expression. Research exploring how UBR4, NAA15 and other ubiquitin ligases affect ICER will provide further insight into the mechanisms involved, now that HA_N-ICER is integrated in the melanoma cell's genome. The ability to control HA_N-ICER expression with dox will show how HA_N-ICER affects melanoma cells, especially regarding protein interactions in the proteasome pathway, as well as apoptosis.

It was previously established that ICER downregulates Bcl-2 expression in myocytes (Tomita et al., 2003). Bcl-2 is an anti-apoptotic protein expressed by the *BCL2* gene, which contains a cAMP response element (CRE) where ICER can bind. If ICER is phosphorylated and either mono- or polyubiquitinated, it may not bind the Bcl-2 promoter, which may contribute to a sustained pro-survival signal in melanoma tumorigenesis. Since HA_N-ICER is more resistant to polyubiquitination due to the presence of the HA tag on the N terminus, experiments may be performed in stable cell lines which will elucidate the interaction between ICER and Bcl-2. The Bcl-2 associated agonist of cell death (Bad) protein, a proapoptotic protein part of the Bcl-2 family of proteins, is inactivated in melanoma cells by the 90kDa ribosomal S6 kinase (RSK) phosphorylation via the MAPK pathway (Eisenmann et al., 2003). Further research would indicate if ICER binding the *BCL2* promoter impacts the pro-apoptotic interaction between Bad and Bcl-2. It is interesting to note that DeGroot et al (2004) identified that the 70kDa RSK phosphorylates CREM in the nucleus; the 90kDA isoform was also analyzed but results were not conclusive at the time. However, RSK proteins clearly affect apoptosis in melanoma cells and

interact with substrates that are involved with or influenced by ICER, and future studies may find a tangible relationship between RSKs and ICER.

Conclusion

This thesis documents that for the first time, a stable cell line expressing HA_N-ICER was generated using cotransfection with a tetracycline-inducible homologous recombinant AAVS1 plasmid and Cas9 gRNA which targets the AAVS1 locus. Through homologous recombination, it was likely incorporated into the AAVS1 locus. The data were confirmed with Western blot analysis and immunocytochemistry. However, sequencing results are needed to verify that HA_N-ICER and EGFP were integrated into the AAVS1 locus. HA_N-ICER, with a decreased turnover rate and increased nuclear localization, will elucidate how it may be used against aggressive, metastatic melanoma in SK-MEL-24 cells. Future experiments will continue to focus on protein interactions, apoptosis, and using HA_N-ICER in drug delivery systems.

Bibliography

American Cancer Society. (2022 January 12). *Key statistics for melanoma skin cancer*. https://www.cancer.org/cancer/melanoma-skin-cancer/about/key-statistics.html

Barrangou, R., Fremaux, C., Deveau, H., Richards, M., Boyaval, P., Moineau, S., Romero, D. A., & Horvath, P. (2007). CRISPR provides acquired resistance against viruses in prokaryotes. *Science (New York, N.Y.)*, *315*(5819), 1709–1712. https://doi.org/10.1126/science.1138140

Bolotin, A., Quinquis, B., Sorokin, A., & Ehrlich, S. D. (2005). Clustered regularly interspaced short palindrome repeats (CRISPRs) have spacers of extrachromosomal origin. *Microbiology (Reading, England)*, *151*(Pt 8), 2551–2561. https://doi.org/10.1099/mic.0.28048-0

Brouns, S. J., Jore, M. M., Lundgren, M., Westra, E. R., Slijkhuis, R. J., Snijders, A. P., Dickman, M. J., Makarova, K. S., Koonin, E. V., & van der Oost, J. (2008). Small CRISPR RNAs guide antiviral defense in prokaryotes. *Science (New York, N.Y.)*, *321*(5891), 960–964. https://doi.org/10.1126/science.1159689

Chacon, A. C., Melucci, A. D., Qin, S. S., & Prieto, P. A. (2021). Thinking small: small molecules as potential synergistic adjuncts to checkpoint inhibition in melanoma. *International journal of molecular sciences*, *22*(6), 3228. https://doi.org/10.3390/ijms22063228

Cirinelli, A., Wheelan, J., Grieg, C., & Molina, C. A. (2022). Evidence that the transcriptional repressor ICER is regulated via the N-end rule for ubiquitination. *Experimental cell research*, *414*(1), 113083. https://doi.org/10.1016/j.yexcr.2022.113083

Davies, H., Bignell, G. R., Cox, C., Stephens, P., Edkins, S., Clegg, S., Teague, J., Woffendin, H., Garnett, M. J., Bottomley, W., Davis, N., Dicks, E., Ewing, R., Floyd, Y., Gray, K., Hall, S., Hawes, R., Hughes, J., Kosmidou, V., Menzies, A., & Futreal, P. A. (2002). Mutations of the BRAF gene in human cancer. *Nature*, *417*(6892), 949–954. https://doi.org/10.1038/nature00766

de Groot, R. P., Ballou, L. M., & Sassone-Corsi, P. (1994). Positive regulation of the cAMP-responsive activator CREM by the p70 S6 kinase: an alternative route to mitogen-induced gene expression. *Cell*, *79*(1), 81–91. https://doi.org/10.1016/0092-8674(94)90402-290k

Deltcheva, E., Chylinski, K., Sharma, C. M., Gonzales, K., Chao, Y., Pirzada, Z. A., Eckert, M. R., Vogel, J., & Charpentier, E. (2011). CRISPR RNA maturation by trans-encoded small RNA and host factor RNase III. *Nature*, *471*(7340), 602–607. https://doi.org/10.1038/nature09886

Eisenmann, K. M., VanBrocklin, M. W., Staffend, N. A., Kitchen, S. M., & Koo, H. M. (2003). Mitogen-activated protein kinase pathway-dependent tumor-specific survival signaling in melanoma cells through inactivation of the proapoptotic protein bad. *Cancer research*, *63*(23), 8330–8337.

Gasiunas, G., Barrangou, R., Horvath, P., & Siksnys, V. (2012). Cas9-crRNA ribonucleoprotein complex mediates specific DNA cleavage for adaptive immunity in bacteria. Proceedings of the National Academy of Sciences of the United States of America, 109(39), E2579–E2586. https://doi.org/10.1073/pnas.1208507109

Healey, M., Crow, M. S., & Molina, C. A. (2013). Ras-induced melanoma transformation is associated with the proteasomal degradation of the transcriptional repressor ICER. *Molecular carcinogenesis*, *52*(9), 692–704. https://doi.org/10.1002/mc.21908

Helmbach, H., Rossmann, E., Kern, M. A., & Schadendorf, D. (2001). Drug-resistance in human melanoma. *International journal of cancer*, *93*(5), 617–622. https://doi.org/10.1002/ijc.1378

Hershko, A., & Ciechanover, A. (1998). The ubiquitin system. *Annual review of biochemistry*, *67*, 425–479. https://doi.org/10.1146/annurev.biochem.67.1.425

Javed, M. R., Sadaf, M., Ahmed, T., Jamil, A., Nawaz, M., Abbas, H., & Ijaz, A. (2018). CRISPR-Cas System: History and Prospects as a Genome Editing Tool in Microorganisms. *Current microbiology*, *75*(12), 1675–1683. https://doi.org/10.1007/s00284-018-1547-4

Jinek, M., Chylinski, K., Fonfara, I., Hauer, M., Doudna, J. A., & Charpentier, E. (2012). A programmable dual-RNA-guided DNA endonuclease in adaptive bacterial immunity. *Science (New York, N.Y.)*, *337*(6096), 816–821. https://doi.org/10.1126/science.1225829

Kim, T. K., & Eberwine, J. H. (2010). Mammalian cell transfection: the present and the future. *Analytical and bioanalytical chemistry*, *397*(8), 3173–3178. https://doi.org/10.1007/s00216-010-3821-6

Krishnan, M., Park, J. M., Cao, F., Wang, D., Paulmurugan, R., Tseng, J. R., Gonzalgo, M. L., Gambhir, S. S., & Wu, J. C. (2006). Effects of epigenetic modulation on reporter gene expression: implications for stem cell imaging. *FASEB journal: official publication of the Federation of American Societies for Experimental Biology*, *20*(1), 106–108. https://doi.org/10.1096/fj.05-4551fje

Kotin, R. M., Linden, R. M., & Berns, K. I. (1992). Characterization of a preferred site on human chromosome 19q for integration of adeno-associated virus DNA by non-homologous recombination. *The EMBO journal*, *11*(13), 5071–5078. https://www.ncbi.nlm.nih.gov/pmc/articles/PMC556985/

Kunin, V., Sorek, R. & Hugenholtz, P. (2007). Evolutionary conservation of sequence and secondary structures in CRISPR repeats. *Genome Biology, 8,* R61. https://doi.org/10.1186/gb-2007-8-4-r61

Lamas, M., Molina, C.A., Foulkes, N.S., Jansen, E., & Sassone-Corsi, P. (1997). Ectopic ICER expression in pituitary corticotroph AtT20 cells: effects on morphology, cell cycle, and hormonal production. *Molecular endocrinology*, *10,* 1425-1434. https://doi.org/10.1210/mend.11.10.9987

Li, J., Poi, M. J., & Tsai, M. D. (2011). Regulatory mechanisms of tumor suppressor P16(INK4A) and their relevance to cancer. *Biochemistry*, *50*(25), 5566–5582. https://doi.org/10.1021/bi200642e

Liang, X., Potter, J., Kumar, S., Zou, Y., Quintanilla, R., Sridharan, M., Carte, J., Chen, W., Roark, N., Ranganathan, S., Ravinder, N., & Chesnut, J. D. (2015). Rapid and highly efficient mammalian cell engineering via Cas9 protein transfection. *Journal of biotechnology*, *208*, 44–53. https://doi.org/10.1016/j.jbiotec.2015.04.024

Lino, C. A., Harper, J. C., Carney, J. P., & Timlin, J. A. (2018). Delivering CRISPR: a review of the challenges and approaches. *Drug delivery*, *25*(1), 1234–1257. https://doi.org/10.1080/10717544.2018.1474964

Marais, R., & Marshall, C. J. (1996). Control of the ERK MAP kinase cascade by Ras and Raf. *Cancer surveys*, *27*, 101–125.

Mémin, E., Genzale, M., Crow, M., & Molina, C. A. (2011). Evidence that phosphorylation by the mitotic kinase cdk1 promotes ICER monoubiquitination and nuclear delocalization. *Experimental cell research*, *317*(17), 2490–2502. https://doi.org/10.1016/j.yexcr.2011.07.001

Molina, C. A., Foulkes, N. S., Lalli, E., & Sassone-Corsi, P. S. (1993). Inducibility and negative autoregulation of CREM: An alternative promoter directs the expression of ICER, an early response repressor. *Cell*, *75*, 875–886. https://doi.org/10.1016/0092-8674(93)90532-u

Nishimasu, H., Ran, F.A.., Hsu, P.D., Ishitani, R., Zhang, F., & Nureki, O. (2014). Crystal structure of cas9 in complex with guide RNA and target DNA. *Cell, 156* (5) 935-949. http://dx.doi.org/10.1016/j.cell.2014.02.001

Poulkes, N.S., Borrelli E., & Sassone-Corsi, P. (1991). CREM gene: use of alternative DNA-binding domains generates multiple antagonists of cAMP-induced transcription. *Cell, 64,* 739-749. https://doi.org/10.1016/0092-8674(91)90503-q

Razavi, R., Ramos, J.C., Yehia, G., Schlotter, F., & Molina, C.A. (1998). ICER-IIγ is a tumor suppressor that mediates the antiproliferative activity of cAMP. *Oncogene, 17,* 3015-3019. https://doi.org/10.1038/sj.onc.1202225

Ruchaud, S., Seite, P., Foulkes, N.S., Sassone-Corsi, P., & Lanotte, M. (1997). The transcriptional repressor ICER and cAMP-induced programmed cell death. *Oncogene, 15*, 827-836. https://doi.org/10.1038/sj.onc.1201248

Sapranauskas, R., Gasiunas, G., Fremaux, C., Barrangou, R., Horvath, P., & Siksnys, V. (2011). The Streptococcus thermophilus CRISPR/Cas system provides immunity in Escherichia coli. *Nucleic acids research*, *39*(21), 9275–9282. https://doi.org/10.1093/nar/gkr606

Stehle, J. H., Foulkes, N. S., Molina, C. A., Simonneaux, V., Pévet, P., & Sassone-Corsi, P. (1993). Adrenergic signals direct rhythmic expression of transcriptional repressor CREM in the pineal gland. *Nature*, *365*(6444), 314–320. https://doi.org/10.1038/365314a0

Tomita, H., Nazmy, M., Kajimoto, K., Yehia, G., Molina, C. A., & Sadoshima, J. (2003). Inducible cAMP early repressor (ICER) is a negative-feedback regulator of cardiac hypertrophy and an important mediator of cardiac myocyte apoptosis in response to beta-adrenergic receptor stimulation. *Circulation research*, *93*(1), 12–22. https://doi.org/10.1161/01.RES.0000079794.57578.F1

Tripathi, R., Liu, Z., Jain, A., Lyon, A., Meeks, C., Richards, D., Liu, J., He, D., Wang, C., Nespi, M., Rymar, A., Wang, P., Wilson, M., & Plattner, R. (2020). Combating acquired resistance to MAPK inhibitors in melanoma by targeting Abl1/2-mediated reactivation of MEK/ERK/MYC signaling. *Nature communications*, *11*(1), 5463. https://doi.org/10.1038/s41467-020-19075-3

Vossler, M. R., Yao, H., York, R. D., Pan, M. G., Rim, C. S., & Stork, P. J. (1997). cAMP activates MAP kinase and Elk-1 through a B-Raf- and Rap1-dependent pathway. *Cell*, *89*(1), 73–82. https://doi.org/10.1016/s0092-8674(00)80184-1

Wiedenheft, B., Sternberg, S. H., & Doudna, J. A. (2012). RNA-guided genetic silencing systems in bacteria and archaea. *Nature, 482*(7385), 331–338. https://doi.org/10.1038/nature10886

Winder, M., & Virós, A. (2018). Mechanisms of drug resistance in melanoma. *Handbook of experimental pharmacology*, *249*, 91–108. https://doi.org/10.1007/164_2017_17

Wu, J., Dent, P., Jelinek, T., Wolfman, A., Weber, M. J., & Sturgill, T. W. (1993). Inhibition of the EGF-activated MAP kinase signaling pathway by adenosine 3',5'-monophosphate. *Science (New York, N.Y.)*, *262*(5136), 1065–1069. https://doi.org/10.1126/science.7694366

Yehia, G., Razavi, R., Memin, E., Schlotter, F., & Molina, C.A. (2001). The expression of inducible cAMP early repressor (ICER) is altered in prostate cancer cells and reverses the transformed phenotype of the LNCaP prostate tumor cell line. *Cancer research, 61*, 6055-6059. https://pubmed.ncbi.nlm.nih.gov/11507053/.

Yehia, G., Schlotter, F., Razavi, R., Alessandrini, A., & Molina, C. A. (2001). Mitogen-activated protein kinase phosphorylates and targets inducible cAMP early repressor to ubiquitin-mediated destruction. *The Journal of biological chemistry*, *276*(38), 35272–35279. https://doi.org/10.1074/jbc.M105404200

Yonish-Rouach, E., Resnitzky, D., Lotem, J., Sachs, L., Kimchi, A., & Oren, M. (1991). Wild-type p53 induces apoptosis of myeloid leukaemic cells that is inhibited by interleukin-6. *Nature*, *352* (6333), 345–347. https://doi.org/10.1038/352345a0.

Zhou, X., Vink, M., Klaver, B., Berkhout, B., & Das, A. T. (2006). Optimization of the Tet-on system for regulated gene expression through viral evolution. *Gene therapy*, *13*(19), 1382–1390. https://doi.org/10.1038/sj.gt.3302780